A biomechanical study of clamping technique on patellar tendon surface strain and material properties using digital image correlation

Colin R. Firminger[1,2,3], W. Brent Edwards[1,2,3]

[1]Human Performance Laboratory, Faculty of Kinesiology, University of Calgary, Canada

[2]Biomedical Engineering Graduate Program, University of Calgary, Canada

[3]McCaig Institute for Bone and Joint Health, University of Calgary, Canada

Corresponding Author: Colin Firminger

Mailing Address: KNB 219, Human Performance Laboratory, University of Calgary, 2500 University Drive NW, Calgary, AB Canada, T2N 1N4

Phone: 403-808-2601

Email: cfirming@ucalgary.ca

Abstract

Several clamping techniques exist for *ex vivo* mechanical testing of tendon. For the patellar tendon, one can choose to clamp directly to the bony attachment sites, the tendon itself, or a combination of the two; however, the influence of these techniques on localized strains and gross material properties is unknown. To this end, uniaxial tensile tests were performed on eleven porcine patellar tendons in three clamping setups while digital image correlation was used to measure axial and transverse strains, Young's modulus, and Poisson's ratio. The setups involved clamping to: 1) the patella and tibia, 2) the patella and the dissected distal tendon, and 3) the dissected proximal and distal tendon. Axial strains in the tendon-tendon clamping setup were 181% higher than patella-tibia clamping (p=0.002) and 131% higher than patella-tendon clamping (p=0.006). Transverse strains were not significantly different between clamping conditions ($p \geq 0.118$). Young's modulus was 50% ($p<0.001$) greater for patella-tibia clamping and 42% ($p<0.001$) greater for patella-tendon clamping when compared to tendon-tendon clamping. For all clamping setups, the tendon illustrated auxetic behavior (i.e., negative Poisson's ratio); however, the Poisson's ratios were 80% smaller in the patella-tibia setup (p=0.006) and 71% smaller patella-tendon setup (p=0.007) compared to the tendon-tendon setup. These results illustrate that discretion should be utilized when reporting material properties derived from mechanical tests involving direct clamping to the dissected patellar tendon at both ends, as this clamping technique significantly increases axial strains, reduces Young's modulus, and alters the tendon's natural auxetic behaviour.

Keywords

Auxeticity; Biomechanics; Strain Concentrations; Young's Modulus

Introduction

Tendons are dense bands of regular connective tissue that transmit tensile loads from muscle to bone, or in the case of the patellar tendon - sometimes referred to as the patellar ligament - bone to bone. Tendons have viscoelastic material properties, and exhibit creep when they are transversely compressed within a clamp.[1] In addition, the outer surface of tendon has a low coefficient of friction to allow for sliding against the synovial sheath that encompasses the tendon.[2,3] This low-friction surface combined with creep during clamping can cause difficulty when creating a solid connection between tendon and actuator for the purpose of mechanical testing.

When clamping directly to tendon, the majority of previous tensile mechanical testing has been accomplished using either compressive or freeze clamps in an attempt to reduce slippage.[4–8] In conjunction with compressive clamps, several techniques have been applied to further reduce slippage, including drying the tendon ends prior to clamping,[9,10] adhering the tendon to the clamp with cyanoacrylate glue,[11,12] or placing sandpaper or cardboard on the inner faces of the clamp. While the aforementioned clamp designs and techniques have proven effective for reducing and/or eliminating slippage, they may cause distortions in the collagen fiber alignment at the interface of the clamp and influence the gross and local mechanical behaviour of the tendon

Several mechanical testing studies have dissected the tendon at the enthesis (i.e., the bony insertion site), creating two tendinous endpoints that must be held during a mechanical test.[13–15] For the patellar tendon, most mechanical testing has been performed by clamping to the bony endpoints (i.e., the patella and tibia), however several studies have also clamped directly to the

tendon.[16–18] Furthermore, direct clamping of the patellar tendon may be necessary to investigate differences in mechanical behaviour between specific anatomical regions, as dissecting the patellar/tibial insertions is not easily facilitated. Direct tendon clamping decreases the aspect ratio (i.e,, length : width) which may increase midsubstance strains due to strain concentrations formed at the clamped ends that can extend well into the unclamped tendon.[19] For the patellar tendon, the effect of clamping to bony versus tendinous endpoints on the mechanical behaviour and surface strains has yet to be investigated.

Digital image correlation (DIC) is a novel methodology for non-invasively quantifying full-field surface strains. Briefly, this technique generates a strain map on the surface of a specimen by tracking the displacement of a stochastic speckle pattern applied to the surface. This approach has been utilized to investigate surface strains on human Achilles tendon and porcine collateral ligaments during tensile mechanical testing.[20,21] By utilizing DIC during mechanical tests of patellar tendon in different clamping setups, the magnitude and size of the strain concentrations near the clamps as well as the midsubstance strains can be evaluated. Additionally, by comparing the nominal strains calculated from both DIC and the actuator crosshead position of the materials testing device, the effect of clamping technique on tendon slippage can be investigated.

The purpose of this study was to examine the effect of three clamping techniques (patella-tibia clamping, patella-tendon clamping, and tendon-tendon clamping) on axial and transverse surface strains, Poisson's ratio, tendon stiffness, and strain concentration size. We hypothesized that direct tendon clamping would significantly decrease tendon stiffness and increase axial/transverse strains and strain concentration size, as the compression of the tendon within the

clamps likely changes the cross section of the tendon from its natural shape, potentially altering its mechanical properties.

Methods

Sample Preparation

Eleven whole patellar tendon samples, still attached to the patella and tibia, were harvested from skeletally mature pigs obtained from a local butcher. Immediately following dissection, samples were wrapped in saline-soaked gauze and stored in a -20°C domestic freezer for a maximum of 2 weeks until testing. Previous literature has shown that the tensile material properties are not significantly different between fresh tendons and those which have undergone a single freeze thaw cycle.[22] On the day of testing, each specimen was thawed for 45 minutes at room temperature while fully submerged in saline. The medial and lateral edges of the patella were removed using a handheld reciprocating bone saw (M.SR-SCT; Foredom, CT, USA) and the posterior face of the patella was trimmed using a diamond-plated precision saw (MC-660; Mark V Laboratory, CT, USA). The bone saw was also used to dissect the tibial tuberosity from the tibia without altering the tibial enthesis of the patellar tendon. An airbrush with a 0.3 mm tip (Master Precision G444; Master Airbrush, China) was used to apply a speckle pattern to the anterior surface of the tendon. Matte black acrylic paint was used to create a high contrast speckle pattern against the white surface of the tendon.

Mechanical Testing and Digital Image Correlation

A series of uniaxial tensile tests were performed in three clamping setups: 1) patella-tibia clamping, 2) patella-tendon clamping, and 3) tendon-tendon clamping. An ElectroPuls E10000

materials testing machine (Instron; MS, USA) was used for all mechanical testing. For the initial (patella-tibia) clamping setup, the patellar and tibial bony endpoints of the tendon were placed into serrated custom clamps. The edges of the clamps were aligned with the tibial and patellar entheses of the tendon to allow for consistent processing of the DIC images. The cross-sectional area of the tendon was assumed to be rectangular and was taken as the average of three locations (proximal, middle, distal), each measured three times using digital calipers while the tendon was loaded to 1 N. Prior to each tensile test, the tendon was preconditioned using a 1 Hz sinusoidal loading pattern to 5 MPa for five cycles to ensure each test had a consistent strain history.[11] Immediately after preconditioning, the tendon was loaded at a rate of 50 $N \cdot s^{-1}$ to a peak load of 9 MPa, which corresponded to 10% of the ultimate tensile strength (UTS) of porcine patellar tendon.[23] This loading magnitude was selected to avoid creating damage in the specimen between the first and third loading protocols. An AVE2 non-contacting video extensometer (Instron, MS, USA) with a measurement accuracy of ±1 μm captured images of the speckle pattern throughout the test at a frequency of 50 Hz. The sample was kept moist throughout the entire testing procedure with a saline drip at a rate of 3 $mL \cdot min^{-1}$.

The patella-tibia tensile test was repeated to assess the reliability of the DIC strain measurement. Following the second patella-tibia test, the distal enthesis was dissected from the tibial tuberosity (patella-tendon setup). A layer of sandpaper was glued to the inner surfaces of the clamp, and the distal 25 mm of tendon was adhered to the sandpaper with cyanoacrylate glue prior to clamping. For the final test, the proximal enthesis was dissected from the patella and placed in a serrated clamp with cyanoacrylate glue and sandpaper as previously mentioned (tendon-tendon setup).

Data Processing and Analysis

Commercially-available software (DIC Replay; Instron, MS, USA) was used to calculate the displacement grid for each test. Raw images (542 × 80 mm) were captured at 50 Hz with a resolution of 0.26 mm/pixel. A user-defined region of interest was created over the tendon, and displacements were calculated using a 31 × 31 pixel subset size to create a displacement grid spacing of 8 × 8 pixels. A strain colourmap of the axial and transverse strain was generated automatically from the displacement grid for each tensile test. Gauge length and midsubstance width were measured from the DIC images. A 9 × 9 pixel Gaussian filter was applied to smooth the strain map, and custom Matlab code (version R2017b; MathWorks, MA, USA) was used to extract axial and transverse strain values for all pixels within the colourmap based on their greyscale value at peak stress. A region-growing algorithm was utilized to segment out the axial strain concentrations near the clamps as follows: starting at the superior/inferior edges of the region of interest, strain concentrations were defined as all adjacent rows containing at least one pixel with a strain value in the upper quartile of the full field strain. For each clamping condition, median and 75^{th} percentile axial and transverse strains were calculated for the entire region of interest, and median and 75^{th} percentile axial strains were also calculated within and outside of the strain concentrations. Furthermore, Poisson's ratio was calculated for each pixel within the filtered strain map as the negative ratio of transverse to axial strain, and the median value was calculated for each clamping condition. Absolute strain concentration length was measured longitudinally as the difference between the maximum and minimum vertical coordinates of all pixels within the strain concentration. In addition, strain concentration length was normalized both as a percentage of the clamped width and as a percentage of the gauge length. Upper and

lower strain concentration lengths were averaged to generate a single value for each clamping type.

In order to measure the effect of each clamping setup on material stiffness, a virtual extensometer was created within DIC Replay that spanned the entire unclamped length of tendon. Nominal strain calculated from the virtual extensometer was compared with crosshead strain calculated from the displacement of the actuator normalized by the gauge length for a given clamping condition to view if clamping type had an effect on the amount of slippage within the clamps. The Young's modulus of each condition was calculated as the slope of the plot of the respective nominal strain (i.e., virtual extensometer or crosshead) versus stress between 50% and 95% of the peak stress to ensure the Young's modulus calculation did not include the toe region of the stress-strain curve. In addition, a virtual extensometer was placed outside of the strain concentrations to obtain a more representative estimate of the tissue's modulus.

Statistical Analysis

The root mean squared coefficient of variation (RMS-CV) was calculated using the median strain to determine the repeatability of strain measurement between the first and second patella-tibia clamping tests. Next, several univariate repeated measures ANOVAs were used to evaluate the effect of each clamping technique on the following variables: DIC-measured gauge length and midsubstance width, median and 75^{th} percentile axial and transverse strains for the entire surface strain map, median and 75^{th} percentile axial strains within and outside of the strain concentrations, Poisson's ratio of the entire strain map, absolute strain concentration length,

strain concentration length normalized to both clamped width and gauge length, and Young's modulus outside of the strain concentrations. A 3 × 2 univariate repeated measures ANOVA (i.e., 3 clamping techniques × 2 nominal strain measurement techniques) was used to investigate the effect of clamping technique on Young's modulus and slippage within the clamps. All statistical tests had an alpha criterion of $\alpha = 0.05$. In the case of a violation of the assumption of sphericity, a Huynh-Feldt correction was used. In the event of a significant effect, Bonferroni post hoc tests were performed to investigate where differences existed. Furthermore, Cohen's *d* values were calculated for any significant differences in the post-hoc tests. All statistical tests were performed in SPSS Statistics 26 (IBM, NY, USA).

Results

The median axial strain RMS-CV was 5.1%, indicating a high degree of reliability in the DIC strain measurement; systematic increases in strain between the first (3.0 ± 0.6%) and second (2.9 ± 0.6%) test, indicative of tendon damage, were not observed. The gauge length and midsubstance width of the tendon in each clamping setup are shown in Table 1. Significant effects of clamping technique were observed for both gauge length ($F(2,20) = 237.2$, $p < 0.001$) and midsubstance width ($F(2,20) = 166.6$, $p < 0.001$). The tendon gauge length significantly decreased from patella-tibia to patella-tendon ($p < 0.001$, $d = -2.56$) and from patella-tendon to tendon-tendon clamping ($p < 0.001$, $d = -3.91$), while the midsubstance width significantly increased from patella-tibia to patella-tendon ($p < 0.001$, $d = 1.38$) and from patella-tendon to tendon-tendon clamping ($p < 0.001$, $d = 2.37$).

A significant effect of clamping technique was observed for median axial strain of the entire surface strain map ($F(1.1, 11.2) = 19.3$, $p = 0.001$, Table 2). Post hoc tests revealed that median axial strain in the tendon-tendon clamping setup was 181% higher than patella-tibia clamping ($p = 0.002$, $d = 1.90$) and 131% higher than patella-tendon clamping ($p = 0.006$, $d = 1.66$). Similarly, a significant effect of clamping technique was observed for 75th percentile strain of the entire strain map ($F(1.2, 12.4) = 22.8$, $p < 0.001$, Table 2). Further, 75th percentile strains in the tendon-tendon setup were 159% greater than the patella-tibia setup ($p = 0.001$, $d = 2.07$) and 115% greater than the patella-tendon setup ($p = 0.003$, $d = 1.85$). Clamping technique also significantly affected median strain within the strain concentration ($F(2,20) = 9.7$, $p = 0.001$), with the median strain during tendon-tendon clamping being 87% greater than patella-tibia clamping ($p = 0.004$, $d = 1.61$). No effect of clamping technique was observed for 75th percentile strains within the strain concentrations ($F(2,20) = 46.7$, $p = 0.226$). Outside of the strain concentrations, axial strains were significantly greater for both the patella-tendon (median: $p = 0.020$, $d = 0.82$; 75th percentile: $p = 0.036$, $d = 0.92$) and tendon-tendon (median: $p = 0.005$, $d = 1.70$; 75th percentile: $p = 0.006$, $d = 1.74$) setups compared to the patella-tibia setup. Post hoc tests showed significant increases in strain outside of the strain concentrations in the tendon-tendon setup compared to the patella-tendon setup for median ($p = 0.021$, $d = 1.45$) and 75th percentile strains ($p = 0.027$, $d = 1.37$). Furthermore, significant effects of clamping technique were not observed for transverse median strain ($F(2,20) = 2.386$, $p = 0.118$), or transverse 75th percentile strain ($F(2,20) = 1.350$, $p = 0.282$).

Median Poisson's ratio was significantly affected by clamping type ($F(1,10) = 9.582$, $p = 0.001$). Poisson's ratio was negative for all three clamping techniques, but the magnitude was 80%

smaller in the patella-tibia setup (p = 0.006, d = 1.94) and 71% smaller patella-tendon setup (p = 0.007, d = 1.57) compared to the tendon-tendon setup.

A significant effect of clamping technique on strain concentration size was observed for the unnormalized measure (F(2,20) = 7.3, p = 0.004), and when normalized by clamp width (F(1.4,14.2) = 19.8, p < 0.001) and gauge length (F(2, 20) = 4.6, p = 0.023). Post hoc tests revealed that the unnormalized strain concentration length was 38% greater for the patella-tibia condition compared to the tendon-tendon condition (p = 0.037, d = 1.34). For the width-normalized measure, the patella-tibia condition was 33% greater than the patella-tendon setup (p = 0.010, d = 1.16) and 57% greater than the tendon-tendon setup (p = 0.002, d = 2.16 respectively). Furthermore, width-normalized strain concentration length was 36% greater for the patella-tendon setup compared to the tendon-tendon setup (p = 0.007, d = 1.95). An opposite trend was observed when the strain concentration lengths were normalized by gauge length, as the tendon-tendon strain concentration was 28% longer than the patella-tendon strain concentration (p = 0.045, d = 1.22).

A linear regression was performed on a representative sample to ensure the region of the stress-strain curve from which Young's Modulus was calculated was indeed linear (see Figure 3). R-squared values of 0.999 were reported for the linear regressions of both the crosshead and virtual extensometer derived strains. No interaction was observed between measurement type (i.e., virtual extensometer versus crosshead) and clamping setup for Young's Modulus values (F(2,60) = 1.0, p = 0.362, Table 3). A significant effect of measurement type on Young's Modulus was observed (F(1,60) = 19.5, p < 0.001), with the virtual extensometer estimating a

35% higher Young's Modulus compared to the crosshead ($p < 0.001$, $d = 1.07$). Clamping type also had a significant main effect on Young's Modulus ($F(2,60) = 25.8$, $p < 0.001$), with post hoc tests revealing that Young's Modulus was 50% greater in the patella-tibia setup ($p < 0.001$, $d = 1.83$) and 42% greater in the patella-tendon setup ($p < 0.001$, $d = 1.49$) compared to the tendon-tendon setup. A significant effect of clamping technique was also observed for Young's modulus calculated outside of the strain concentrations ($p = 0.041$, Table 3), with a trend for reduced Young's modulus in the tendon-tendon compared to the patella-tibia setup ($p = 0.091$, $d = -1.06$).

Discussion

The purpose of this study was to investigate the effect of clamping technique on patellar tendon surface strains, strain concentration size, and tendon stiffness. Clamping technique had a significant effect on median and 75th percentile strains for the entire strain map, as well as absolute and normalized strain concentration size. Within the strain concentrations, a significant main effect of clamping technique was only observed for median strain. Clamping technique also significantly affected tendon stiffness, as Young's modulus was significantly lower in the tendon-tendon condition compared to the patella-tendon and patella-tibia conditions. Post hoc tests of all significant strain and stiffness measures revealed that patella-tibia and patella-tendon clamping were not significantly different, except for the strain concentration size normalized to clamp width, Poisson's ratio, and axial strain outside of the strain concentrations. While some differences exist, these results indicate that for the patellar tendon, the combination of clamping to the patella and tendon does not substantially alter the mechanical behaviour when compared to clamping to the patella and tibia. On the other hand, clamping to the patellar tendon at both ends significantly reduces stiffness and increases median and 75th percentile axial strain.

When a tendon is loaded in tension, collagen fibers are first recruited and begin to lengthen and slide relative to one another.[24–26] Once strains increase beyond 6%, interfiber and intermolecular crosslinks begin to break and fibers begin to fail, causing the load to be transferred to the remaining intact fibers and initiating the failure of the entire tendon.[25] Previously reported monotonic failure strains have ranged from 5.1%-16.3%.[27–32] These studies used a variety of different clamping setups, therefore we speculate that some of the observed variance in ultimate failure strain could be due to clamping technique rather than differences between the tendons themselves. In this study, median strains were 2.8 times higher (8.2% vs. 2.9%) for tendon-tendon clamping than patella-tibia clamping. Based on these results, utilizing tendon-tendon clamping for ultimate tensile testing of small aspect ratio tendons may underestimate failure strain if nominal measures are used. However, clamping tendon at one end did not significantly increase median or 75th percentile strains compared to patella-tibia clamping. This finding is important as the majority of tendons originate in muscle and insert into bone, and tensile testing must occur with at least one end clamped directly to the tendon.

For a given isotropic material under load, stress concentrations will exist near the point of load application and, according to Saint Venant's principle, extend into the body at a distance approximately equal to the largest dimension of the body's cross-section in contact with the applied load. This effect is magnified for a highly anisotropic materials such as tendon, as strain concentration lengths can be in excess of ten times the clamped width.[19] The use of digital image correlation allowed us to measure the magnitude and size of the strain concentrations that existed near the clamps, which were arbitrarily defined as all contiguous rows containing a pixel with an

axial strain greater than the 75th percentile strain of the entire strain map. Within the strain concentrations, median axial strains were significantly higher when clamping directly to both sides of the tendon than to one side of the tendon or bone-to-bone. Furthermore, median and 75th percentile axial strains outside of the strain concentrations (i.e., the tendon midsubstance) were significantly greater in the patella-tendon and tendon-tendon setups compared to the patella-tibia setup, as well as between the patella-tendon and tendon-tendon setups. Previous tendon mechanical testing studies have recommended an aspect ratio of 4:1 such that midsubstance strains are not affected by strain concentrations.[33] We observed aspect ratios of 3.6:1 and 1.1:1 in the patella-tendon and tendon-tendon setups, respectively, which support our observations of increased axial strains located in the midsubstance as the strain concentrations likely were not able to be dissipated adequately at the tendon midsubstance. If the strain concentrations are not accounted for, the increased strains generated within the tendon during patella-tendon and tendon-tendon clamping may be falsely interpreted as a lower nominal failure strain.

While the increased midsubstance strains observed in tendon-tendon clamping may be partly due to the strain concentrations extending into the tissue, removing the enthesis from the tendon may also play a large role. Entheses are highly specialized regions in which fibrils insert into bone over a distance of 130 μm,[34] and strain concentrations have been observed at the calcaneal enthesis during tensile testing of Achilles tendon.[28] The patellar tendon is highly adapted to transmit load from the patella to the tibia, and moving the point of highest strain from the enthesis to the midsubstance likely hinders the tendon's ability to resist as much tensile load. Furthermore, the transverse compression within the clamps causes distortion of the tendon fibers, likely increasing the shear stress near the clamps as well. This novel loading environment may

313 break some of the intra-fibrillar attachments which have been known to resist fiber sliding as the
314 tendon is loaded, further weakening the tendon's ability to resist tensile load. The combination of
315 a novel loading environment, altered cross-section, and strain concentrations to a poorly adapted
316 part of the tendon act to weaken the tendon's Young's modulus and increase the midsubstance
317 strains observed for a given stress.
318
319 In terms of tendon stiffness, no interaction was observed between strains calculated with the
320 virtual extensometer versus the crosshead displacement. This lack of an interaction illustrates
321 that the tendon was not slipping more in the tendon-tendon clamping condition when compared
322 to the patella-tibia or patella-tendon clamping conditions. A significant main effect of
323 measurement type was observed for Young's modulus. We speculate that significantly lower
324 Young's modulus measured using crosshead displacement was mainly caused by slippage of the
325 tendon in the clamps, and to a lesser degree, the laxity in the loading frame. Furthermore,
326 Young's modulus was significantly lower for tendon-tendon clamping compared to both patella-
327 tibia and patella-tendon clamping, while no difference was observed between the patella-tibia
328 and patella-tendon clamping. When directly clamped, the lower Young's modulus was likely due
329 to a combination of the clamp weakening the tendon structure and the short aspect ratio not
330 allowing the strain concentrations to fully dissipate over the short length of the tissue. Therefore,
331 strains were likely naturally higher for the same axial load, leading to a lower apparent modulus.
332 This is further evidenced by the significant effect of clamping technique on Young's modulus
333 measured outside of the strain concentrations. These findings complement the strain map results,
334 showing that direct tendon clamping at both ends weakens the tendon while clamping to bone at
335 one end and tendon at the other does not significantly alter tendon stiffness.

We discovered porcine patellar tendons exhibited a negative Poisson's ratio in the frontal plane. This behaviour, commonly known as auxeticity, indicated that the tendon is widening in the transverse direction as it elongates in the longitudinal direction. While this behaviour seems counterintuitive for tendon, it may be explained by tendon's gross shape in the frontal plane. The porcine patellar tendons displayed a curved, waisted geometry, whereby the patellar and tibial entheses were wider than the tendon midsubstance. As the tendon was loaded, the curved geometry changed to a more fan-like, straight geometry, likely because the individual fibers were straightened in a direct line connecting their tibial and patellar insertions (see Figure 4). As such, the observed auxetic behaviour in the frontal plane is more indicative of a structural or geometric phenomenon rather than a unique material property. These findings are supported by previous research on Achilles tendon, which also reported auxetic behaviour in the frontal plane during uniaxial tensile loading.[35] Our results also illustrated that clamping technique affected the degree of auxeticity displayed in the frontal plane, as direct tendon clamping likely altered the orientation of the collagen fibers at the clamp and created a more uniform width throughout the sample. The Poisson's ratio when clamping directly to the tendon ends was reduced by 80% (from -1.39 to -0.28) compared to patella-tibia clamping, and by 71% compared to patella-tendon clamping (from -0.95 to -0.28). While the Poisson's ratio in the tendon-tendon clamping condition was still auxetic, this significant reduction further indicates that tendon-tendon clamping is likely not representative of the structural and material behaviour of the patellar tendon when it is clamped at the patella and tibia.

One main limitation with this research was that the same sample was used consecutively in the three clamping setups, introducing the possibility that the sample may accrue damage throughout the testing procedure that may falsely inflate the observed strains in the second and third clamping setups. The high degree of repeatability and lack of systematic increase in strain between the first and second patella-tibia tests increases our confidence that the tendon was not being damaged. Furthermore, using a fatigue life relationship developed from cyclically-loaded human extensor digitorum longus tendons, our samples should theoretically be able to withstand 2.5 million cycles prior to failure when loaded at 10% UTS.[36] Thus, we are confident that the 24 total cycles (20 of which were at 5% UTS) did not damage the tendon in a meaningful way. Another limitation associated with this research was that only anterior surface strains were able to be measured with the tendon in full extension. One finite element modeling study suggested that a strain concentration may exist below the tendon surface at the inferior patellar pole,[37] while several *in vitro* studies reported differences in anterior versus posterior strains with knee angle and location-dependent fascicle material properties.[11,38,39] Using DIC to investigate the effect of knee flexion on both anterior and posterior patellar tendon strains may therefore be an important future direction. Furthermore, future work on the Poisson's ratio in the sagittal plane would be beneficial to investigate whether it exhibits the auxetic behaviour we observed in the frontal plane. Of course, our findings are specific to the patellar tendon of skeletally mature pigs obtained from a local butcher and may need to be verified for other tendons and animals.

Conclusion

This study used digital image correlation to assess the effect of clamping technique on anterior surface patellar tendon strains. We found that clamping directly to the patellar tendon at the

proximal and distal ends significantly increased median and 75th percentile strains and significantly decreased Young's modulus and Poisson's ratio compared to clamping at the bony endpoints and when clamping at the patella and distal tendon. These results indicate that for the patellar tendon or tendons with low aspect ratios, caution should be exercised when reporting tendon material properties obtained from material tests involving direct tendon clamping, as this setup has been shown to increase strains and weaken the patellar tendon compared to the idealized setup of clamping to both bony endpoints.

Acknowledgements

Funding for this research was provided in part by the Natural Sciences and Engineering Research Council of Canada (NSERC; RGPIN 01029-2015, CGSD3 504212-2017) and from an Alberta Innovates Graduate Studentship. Research infrastructure for this study was funded by a Canadian Foundation for Innovation (CFI) John R. Evans Leaders Fund (JELF; project #37134).

References

1. Buckley CP, Salisbury STS, Zavatsky AB. 2016. Viscoelasticity of tendons under transverse compression. J. Biomech. Eng. 138(10):1–8.
2. Uchiyama S, Coert JH, Berglund L, et al. 1995. Method for the measurement of friction between tendon and pulley. J. Orthop. Res. 13(1):83–89.
3. Amadio PC. 2012. Friction of the gliding surface: Implications for tendon surgery and rehabilitation. J. Hand Ther. 18(2):112–119.
4. Shi DF, Wang DM, Wang CT, Liu A. 2012. A novel, inexpensive and easy to use tendon clamp for in vitro biomechanical testing. Med. Eng. Phys. 34(4):516–520.
5. Cheung JTM, Zhang M. 2006. A serrated jaw clamp for tendon gripping. Med. Eng. Phys. 28(4):379–382.
6. Sharkey NA, Smith TS, Lundmark DC. 1995. Freeze clamping musculo-tendinous junctions for in vitro simulation of joint mechanics. J. Biomech. 28(5):631–635.
7. Riemersa DJ, Schamhardt HC. 1982. The cryo-jaw, a clamp designed for in vitro rheology studies of horse digital flexor tendons. J. Biomech. 15(8):619–620.
8. Schechtman H, Bader DL. 2002. Fatigue damage of human tendons. J. Biomech. 9290(97):347–353.
9. Haut RC. 1983. Age–dependent influence of strain rate on the tensile failure of rat–tail tendon. J. Biomech. Eng. 105(3):296–299.
10. Wang XT, Ker RF. 1995. Creep rupture of wallaby tail tendons. J. Exp. Biol. 198:831–845.
11. Haraldsson BT, Aagaard P, Krogsgaard M, et al. 2005. Region-specific mechanical properties of the human patella tendon. J. Appl. Physiol. 98:1006–1007.

12. Shadwick RE. 1990. Elastic energy storage in tendons: Mechanical differences related to function and age. J. Appl. Physiol. 68(3):1033–1040.

13. Lynch HA, Wu JP, Elliott DM. 2003. Effect of Fiber Orientation and Strain Rate on the Nonlinear Uniaxial Tensile Material Properties of Tendon.125(October).

14. Hubbard RP, Soutas-Little RW. 1984. Mechanical properties of human tendon and their age dependence. J. Biomech. Eng. 106(2):144–50 Available from: http://www.ncbi.nlm.nih.gov/pubmed/6738019.

15. Wang XT, Ker RF, Alexander RM. 1995. Fatigue rupture of wallaby tail tendons. J. Exp. Biol. 198:847–852 Available from: http://jeb.biologists.org/content/198/3/831.long.

16. Ristaniemi A, Stenroth L, Mikkonen S, Korhonen RK. 2018. Comparison of elastic, viscoelastic and failure tensile material properties of knee ligaments and patellar tendon. J. Biomech. Available from: https://linkinghub.elsevier.com/retrieve/pii/S0021929018306134.

17. Stäubli HU, Schatzmann L, Brunner P, et al. 1999. Mechanical tensile properties of the quadriceps tendon and patellar ligament in young adults. Am. J. Sports Med. 27(1):27–34.

18. Beynnon BD, Proffer D, Drez DJ, et al. 1995. Biomechanical Assessment of the Healing Response of the Rabbit Patellar Tendon After Removal of Its Central Third. Am. J. Sports Med. 23(4):452–457.

19. Horgan CO, Simmonds JG. 1994. Saint-Venant end effects in composite structures. Compos. Eng. 4(3):279–286.

20. Luyckx T, Verstraete M, De Roo K, et al. 2014. Digital image correlation as a tool for three-dimensional strain analysis in human tendon tissue. J. Exp. Orthop. 1(7):7 Available from: http://www.jeo-esska.com/content/1/1/7.

21. Lionello G, Sirieix C, Baleani M. 2014. An effective procedure to create a speckle pattern on biological soft tissue for digital image correlation measurements. J. Mech. Behav. Biomed. Mater. 39:1–8 Available from: http://dx.doi.org/10.1016/j.jmbbm.2014.07.007.
22. Huang H, Zhang J, Sun K, et al. 2011. Effects of repetitive multiple freeze-thaw cycles on the biomechanical properties of human flexor digitorum superficialis and flexor pollicis longus tendons. Clin. Biomech. 26(4):419–423 Available from: http://dx.doi.org/10.1016/j.clinbiomech.2010.12.006.
23. Ringer GW. 1998. Mechanical Characteristics of Porcine Patellar Tendons.
24. Mosler E, Folkhard W, Knörzer E, et al. 1985. Stress-induced molecular rearrangement in tendon collagen. J. Mol. Biol. (182):589–596.
25. Screen HRC, Lee DA, Bader DL, Shelton JC. 2004. An investigation into the effects of the hierarchical structure of tendon fascicles on micromechanical properties. Proc. Inst. Mech. Eng. Part H J. Eng. Med. 218(2):109–119.
26. Maganaris C, Narici M. 2005. Mechanical properties of tendons. In: Maffulli N, Renstrom P, Leadbetter W, editors. Tendon Injuries. London: Springer. p 385–396.
27. Yamamoto N, Hayashi K. 1992. Mechanical properties of collagen fascicles from the rabbit patellar tendon. J. Biomech. Eng. 114:332–337.
28. Wren TAL, Yerby SA, Beaupré GS, Carter DR. 2001. Mechanical properties of the human achilles tendon. Clin. Biomech. 16(3):245–251.
29. Johnson GA, Tramaglini DM, Levine RE, et al. 1994. Tensile and viscoelastic properties of human patellar tendon. J. Orthop. Res. 12(6):796–803 Available from: http://www.ncbi.nlm.nih.gov/pubmed/7983555.
30. Butler D, Grood ES, Noyes FR, et al. 1984. Effects of structure and strain measurement

technique on the material properties of young human tendons and fascia. J. Biomech. 17(8):579–596.

31. Nakagawa Y, Hayashi K, Yamamoto N, Nagashima K. 1996. Age-related changes in biomechanical properties of the Achilles tendon in rabbits. Eur. J. Appl. Physiol. Occup. Physiol. 73:7–10.

32. Butler D, Kay M, Stouffer D. 1986. Comparison of Material Properties in Fascicle-Bone Units From Human Patellar Tendon and Knee Ligaments. J. Biomech. 19(6):425–432.

33. Elliott DM, Leroux MA, Laursen TA, Setton LA. 1997. Formulation of a Continuum Anisotropic Model for the Annulus Fibrosus in Tension. Adv. Bioeng. ASME BED 36:165–166.

34. Gao J, Messner K. 1996. Quantitative comparison of soft tissue-bone interface at chondral ligament insertions in the rabbit knee joint. J. Anat. 188(2):367–373.

35. Gatt R, Vella Wood M, Gatt A, et al. 2015. Negative Poisson's ratios in tendons: An unexpected mechanical response. Acta Biomater. 24:201–208 Available from: http://dx.doi.org/10.1016/j.actbio.2015.06.018.

36. Schechtman H, Bader DL. 1997. In vitro fatigue of human tendons. J. Biomech. 30(8):829–835.

37. Lavagnino M, Arnoczky SP, Elvin N, Dodds J. 2008. Patellar Tendon Strain is Increased at the Site of the Jumper's Knee Lesion during Knee Flexion and Tendon Loading: Results and Cadaveric Testing of a Computational Model. Am. J. Sports Med. 36(11):2110–2118 Available from: http://journals.sagepub.com/doi/10.1177/0363546508322496.

38. Almekinders LC, Vellema JH, Weinhold PS. 2002. Strain patterns in the patellar tendon

and the implications for patellar tendinopathy. Knee Surgery, Sport. Traumatol. Arthrosc. 10(1):2–5.

39. Basso O, Amis AA, Race A, Johnson DP. 2002. Patellar tendon fiber strains: their differential responses to quadriceps tension. Clin. Orthop. Relat. Res. (400):246–253.

Tables

Table 1: Average (SD) tendon dimensions for each clamping setup measured from DIC images

Clamping Setup	Gauge length (mm)	Midsubstance width (mm)
Patella-Tibia	71.14 (5.13)	15.49 (1.82)
Patella-Tendon	54.66 (7.52)[a]	18.23 (2.12)[a]
Tendon-Tendon	27.38 (6.38)[a,b]	24.11 (2.79)[a,b]
p-value	<0.001	<0.001

[a]Significantly different from Patella-Tibia Clamp ($p < 0.050$), [b]Significantly different from Patella-Tendon Clamp ($p < 0.050$)

Table 2: Effect of clamping setup on average (SD) surface axial and transverse strain distribution, strain concentration size, and Poisson's ratio

	Entire Surface					Strain Concentrations					Outside of Strain Concentrations (Midsubstance)	
	Axial Strain		Transverse Strain			Axial Strain					Axial Strain	
	Median (%)	75th Percentile (%)	Median (%)	75th Percentile (%)	Median Poisson's Ratio	Median (%)	75th Percentile (%)	Length (mm)	Length (% clamped width)	Length (% gauge length)	Median (%)	75th Percentile (%)
Patella-Tibia Clamp	2.91 (0.65)	5.31 (1.69)	5.02 (2.50)	9.94 (3.29)	-1.39 (0.75)	7.40 (3.54)	16.10 (6.75)	10.04 (3.90)	51.48 (19.14)	17.69 (6.52)	2.15 (0.53)	3.35 (0.58)
Patella-Tendon Clamp	3.53 (0.82)	6.39 (1.12)	3.80 (2.37)	7.80 (3.30)	-0.95 (0.54)	8.85 (2.95)	16.75 (4.07)	8.11 (1.63)	34.31 (8.58)[a]	17.66 (4.02)	2.65 (0.67)[a]	4.11 (1.02)[a]
Tendon-Tendon Clamp	8.17 (3.87)[a,b]	13.74 (5.52)[a,b]	2.75 (2.40)	2.75 (2.40)	-0.28 (0.28)[a,b]	13.81 (4.37)[a]	19.95 (5.57)	6.20 (1.13)[a]	21.95 (2.60)[a,b]	24.53 (6.90)[b]	5.75 (2.93)[a,b]	7.45 (3.28)[a,b]
p-value	0.001	<0.001	0.118	0.282	0.001	0.001	0.226	0.004	<0.001	0.023	0.003	0.003

[a]Significantly different from Patella-Tibia Clamp ($p < 0.050$), [b]Significantly different from Patella-Tendon Clamp ($p < 0.050$).

Table 3: Estimates of Average (SD) Young's modulus using virtual extensometer versus crosshead data

		Young's Modulus (MPa)	
		Strain concentrations included	Strain concentrations removed
Measurement Type	Virtual Extensometer	263.4 (53.8)	-
	Crosshead Displacement	172.1 (31.9)	-
	p-value	<0.001	-
Clamping Setup	Patella-Tibia Clamp	278.4 (61.6)	526.7 (228.7)
	Patella-Tendon Clamp	237.0 (55.4)	454.9 (287.9)
	Tendon-Tendon Clamp	137.9 (35.4)[a,b]	311.5 (175.6)
	p-value	<0.001	0.041
	Interaction p-value	0.158	-

[a]Significantly different from Patella-Tibia Clamp ($p < 0.050$), [b]Significantly different from Patella-Tendon Clamp ($p < 0.050$)

503 **Figures**

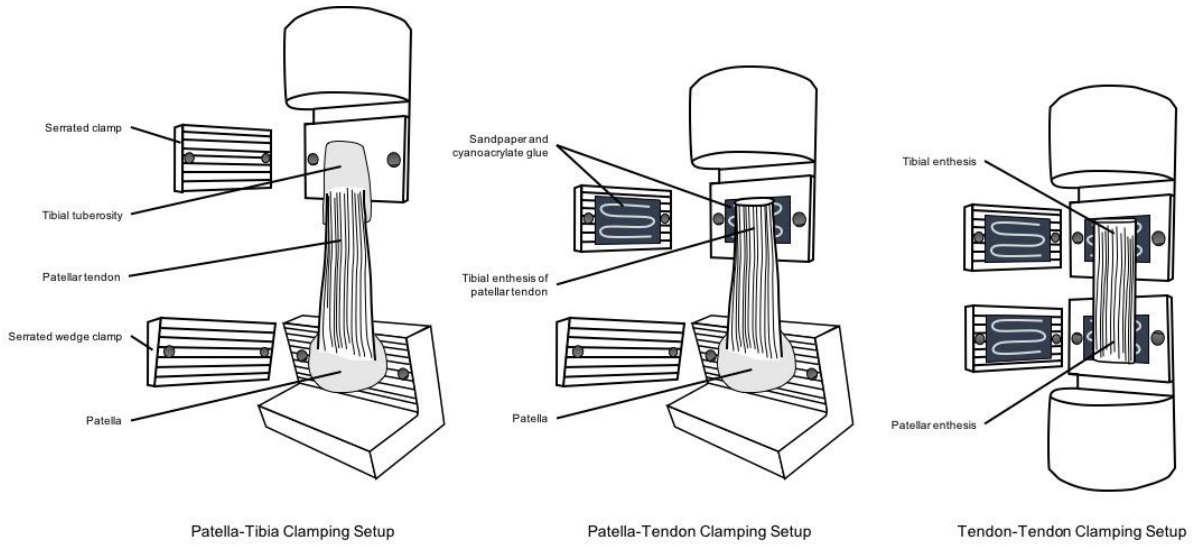

504

505 Figure 1: Schematics of each clamping setup

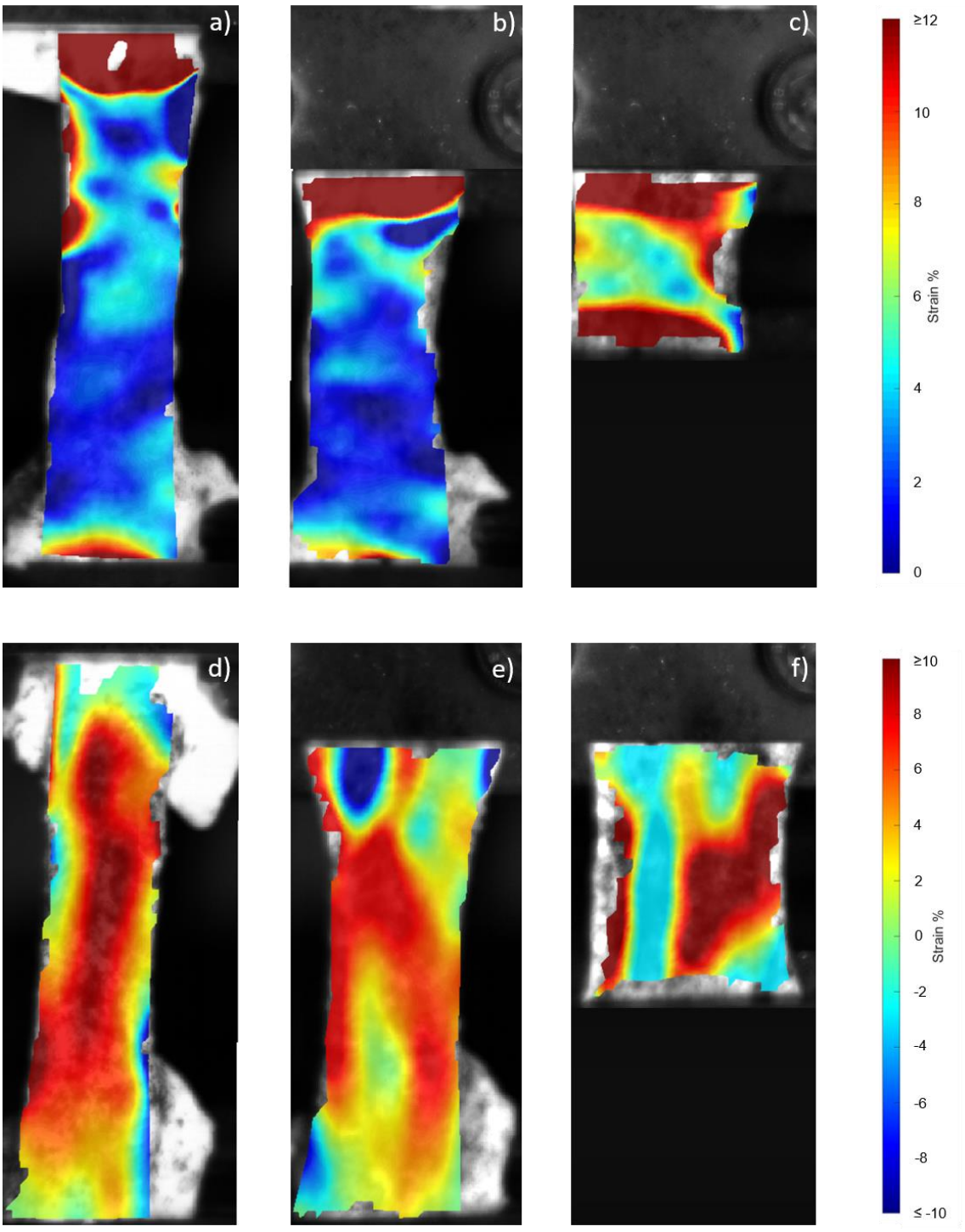

506

507 Figure 2: Representative strain maps for each clamping setup. Top row shows axial strain while

508 bottom row shows transverse strain. Panels a),d): patella-tibia clamping; panels b), e): patella-

509 tendon clamping; panels c), f): tendon-tendon clamping.

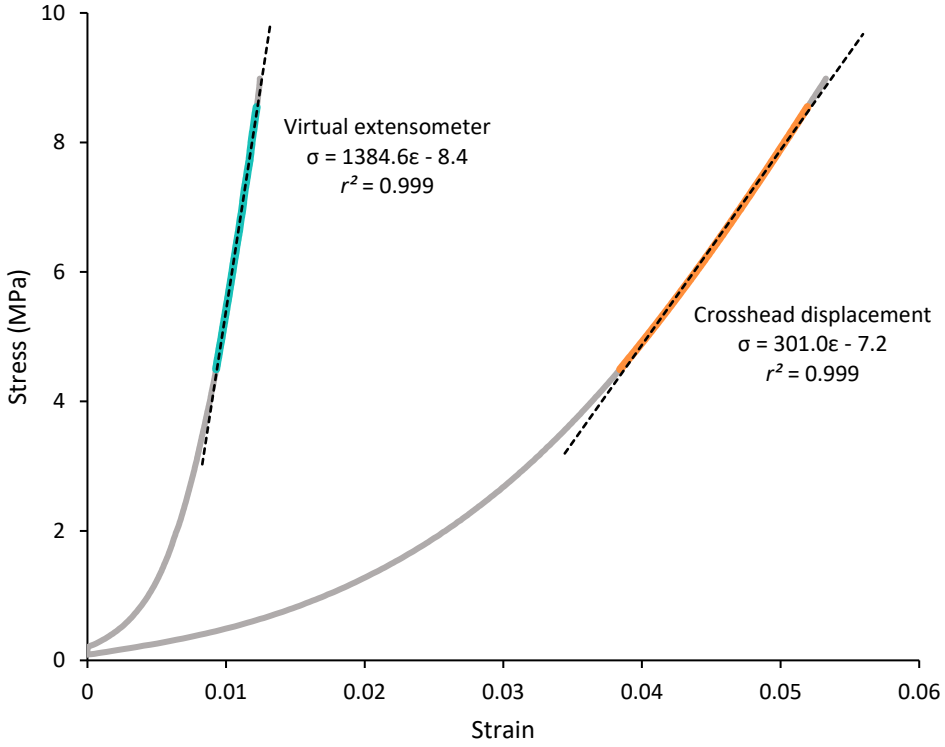

Figure 3: Stress-strain curves of a representative sample derived from a virtual extensometer and crosshead displacement. Coloured regions represent 50-95% of peak stress, and the dotted black lines represent the linear regression fitted to the coloured region.

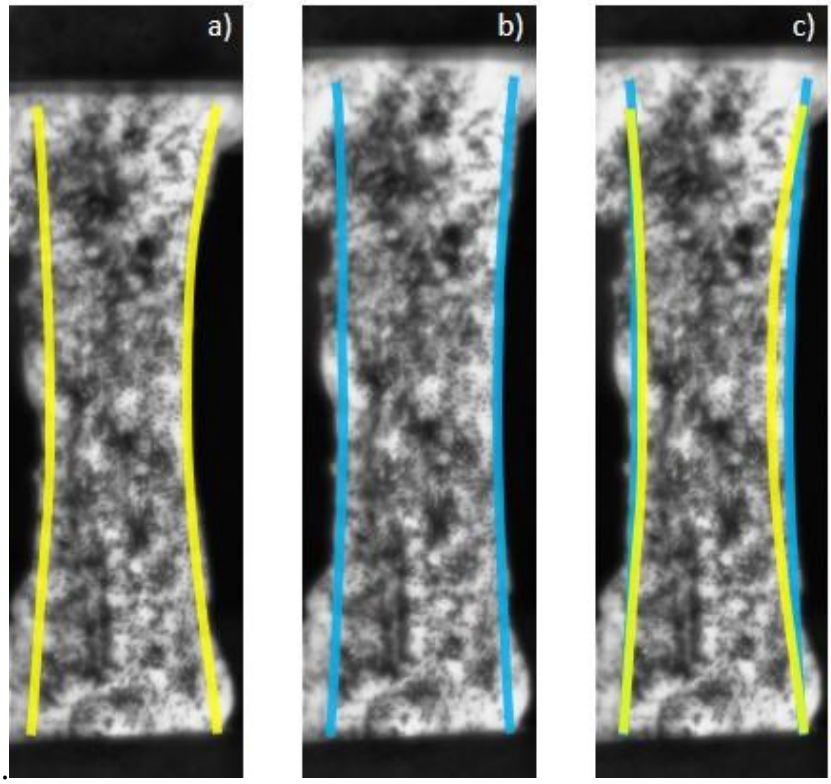

516 .

517 Figure 4: The gross frontal profile of a representative sample at: a) zero load; b) peak load (9

518 MPa); c) peak load with the unloaded profile overlaid